

Control-Matrix Approach to NCSX Design

H. Mynick, N. Pomphrey
PPPL

1999 Meeting of the APS/DPP
Seattle, WA, Nov. 15–19, 1999

The control matrix (CM) approach yields a description of the combinations of knobs Z_j which can be adjusted to provide independent control of physics figures of merit P_i (*e.g.*, ripple levels or kink growth rates), as well as those combinations which affect none of these P_i . This can be used both in finding superior design points, as well as in using a configuration's control knobs to have good operational flexibility about those design points.

Acknowledgements: L.P. Ku, A.H. Boozer

● Motivation:

In developing candidate QAS configurations,¹ the NCSX group has relied heavily on an automated optimizer, which conducts a search in a parameter space $\mathbf{Z} = \{Z_j\} (j = 1, \dots, N_z)$ describing the stellarator boundary, using an objective function $F(P)$, a function of figures of merit $\mathbf{P} = \{P_i(\mathbf{Z})\} (i = 1, \dots, M_p)$ characterizing the physics properties (*e.g.*, transport, kink stability, *etc.*) of the configuration. While a powerful tool, the optimizer is searching a space whose topography has been essentially unknown, and we have rather limited understanding of why the optimizer arrives at the design points \mathbf{Z}_0 it does. For example, what are the essential features of the shape that are responsible for the desired physics properties? Deeper insight into this would enhance our ability to locate attractive design points, and understand the effect of perturbations from those points.

The control matrix (CM) project is intended to provide this insight, through increased understanding of the topography, and through applying mathematical techniques such as SVD methods to gain a clear grasp of how the $P_i(\mathbf{Z})$ can be changed to achieve superior base configurations and operational flexibility.

● Formulation:

● We consider 2 linearly-related ‘configuration spaces’ \mathbf{X} and \mathbf{Z} specifying a stellarator:

● The ‘full-space’ \mathbf{X} of coefficients

$$\mathbf{X} \equiv \{X_{j=1, \dots, N_x}\} \equiv (R_{\mathbf{m}_1}, Z_{\mathbf{m}_1}, R_{\mathbf{m}_2}, \dots, Z_{\mathbf{m}_{N_x/2}})$$

needed for (*e.g.*) a VMEC equilibrium specification of the boundary. Here, $\mathbf{m} \equiv (\tilde{n} \equiv n/N_{fp}, m)$, and $N_x \sim 70$.

● The ‘reduced-space’ \mathbf{Z} of combinations of those X_j which capture the most important physics:

$$\mathbf{Z} \equiv \{Z_{j=1, \dots, N_z}\}, \text{ where } N \equiv N_z \leq N_x.$$

● Over \mathbf{X} or \mathbf{Z} , we consider the behavior of $M \equiv M_p \sim 5$ physics figures of merit

$$\mathbf{P} \equiv \{P_i(\mathbf{Z})\} = (\chi_1^2, \chi_2^2, W_1, W_2, \lambda), \text{ where:}$$

· $P_5 \equiv \lambda =$ kink eigenvalue (from TERPSICHORE), and P_{1-4} are 4 measures of the ripple, hence of the

level of nonaxisymmetric transport one might expect:

$$P_{1,2} \equiv \chi_{1,2}^2 \equiv \chi^2(\psi_{1,2}) \equiv N_{\mathbf{m}}^{-1} \sum_{m, \tilde{n} \neq 0} B_{\mathbf{m}}^2 / B_0^2, \text{ with } \psi \text{ the toroidal flux, } = \psi_a \text{ at the edge, and } \psi_1 / \psi_a = 1/4, \psi_2 / \psi_a = 1/2.$$

· $P_{3,4} \equiv W_{1,2}$ is the ‘water function’² at $\psi_{1,2}$, measuring how deep the ripple wells are over a flux surface.

• Expand $\mathbf{P}(\mathbf{Z} = \mathbf{Z}_0 + \mathbf{z}) = \mathbf{P}(\mathbf{Z}_0) + \mathbf{p}$ about $\mathbf{Z} = \mathbf{Z}_0$. One has (writing in component-form, with summation over repeated indices assumed)

$$p_i(\mathbf{Z}_0 + \mathbf{z}) = G_{ij}(\mathbf{Z}_0)z_j + \frac{1}{2}H_{ijk}(\mathbf{Z}_0)z_jz_k + (h.o.), \quad (1)$$

\uparrow 'control matrix' \nwarrow 'Hessian'

with $h.o. \equiv$ higher-order terms. For small enough \mathbf{z} , one has matrix equation

$$\mathbf{p} = \mathbf{G}_0 \cdot \mathbf{z}, \quad (2)$$

with $\mathbf{G}_0 \equiv \mathbf{G}(\mathbf{Z}_0)$ the $M \times N$ 'control matrix' at design point \mathbf{Z}_0 . It may be inverted, using the SVD theorem

$$\mathbf{G}_{M \times N} = \mathbf{U}_{M \times N} \cdot \mathbf{W}_{N \times N} \cdot \mathbf{V}_{N \times N}^T,$$

with \mathbf{U}, \mathbf{V} unitary matrices, and \mathbf{W} a diagonal matrix.

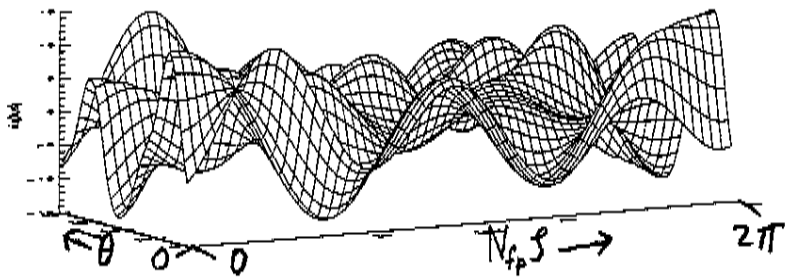
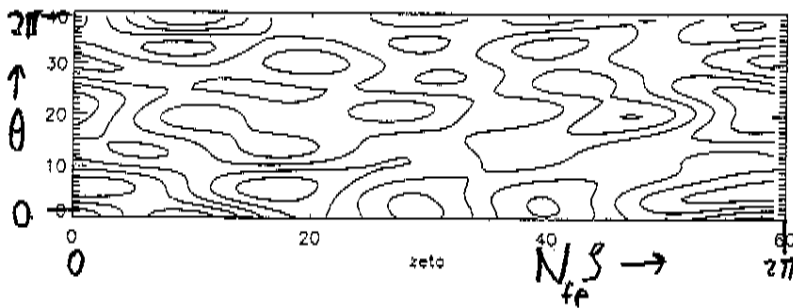
• Taking the particular basis set $\pi^{i=1,M}$ which have 1 in the i^{th} position and 0 elsewhere, one has the corresponding set ξ^i of displacements

$$\xi^i \equiv \mathbf{G}_0^{-1} \cdot \pi^i,$$

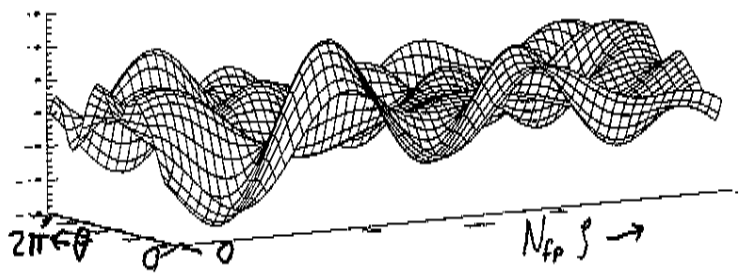
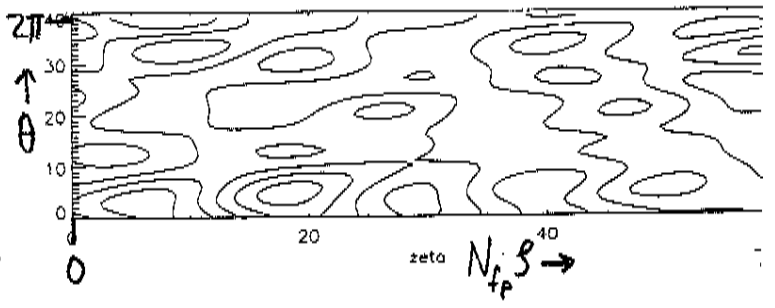
physically representing a set of displacements which vary a single physics parameter P_i , leaving the others unchanged. These span the 'range' of \mathbf{G} . The $(N - M)$ vectors spanning the nullspace of \mathbf{G} (change the configuration without modifying any of the P_i) are also important. To begin, we look at the ξ^i .

- c10 : Initial results, for $Z = X$, $N_z = N_x$:
 (A) 'More-constrained' case ($M_p = 5$).
 • Plot $\xi^i(\theta, \zeta) \equiv \xi_R^i + \xi_z^i$ to assess the ξ^i :

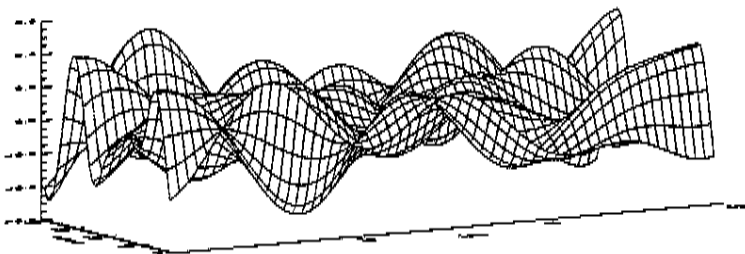
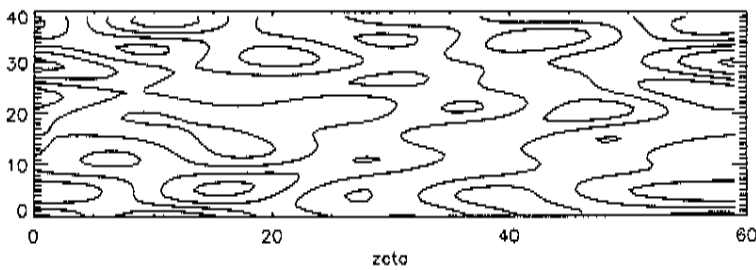
$i=1$ (χ_1^2)



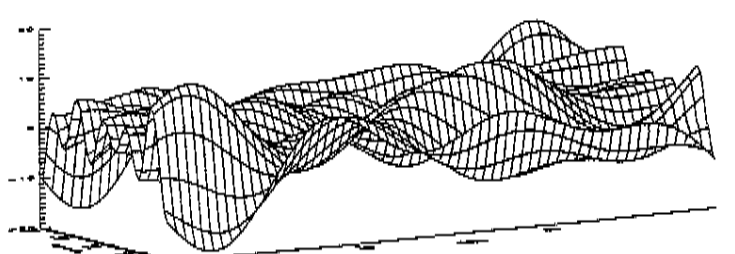
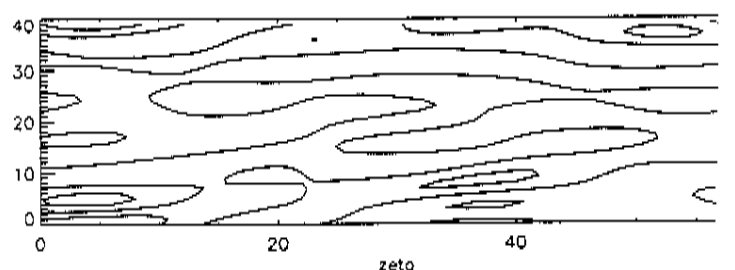
$i=2$ (χ_2^2)



$i=4$ (W_2)



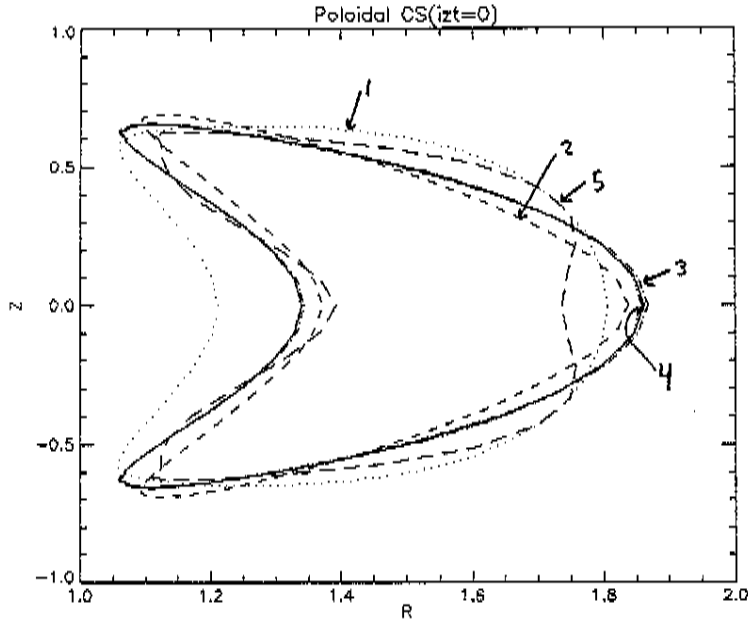
$i=5$ (λ -kink)



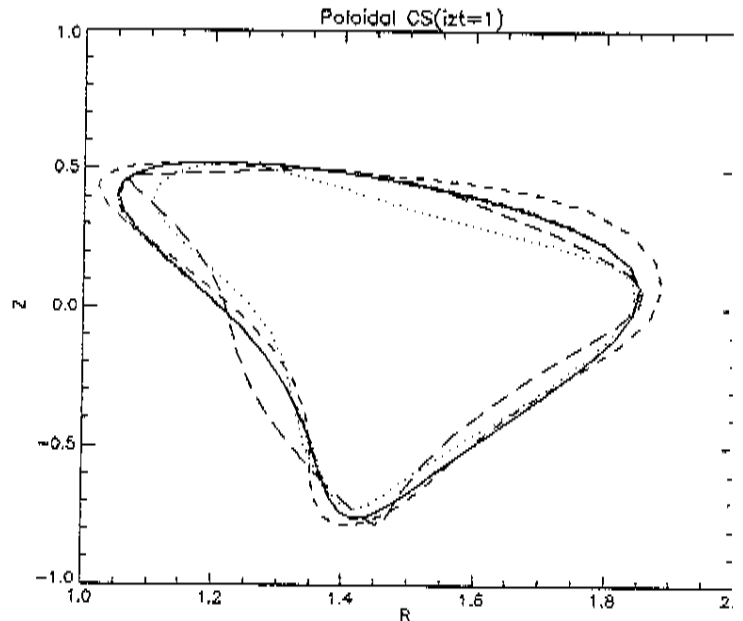
(A), cont:

• Surface deformations:

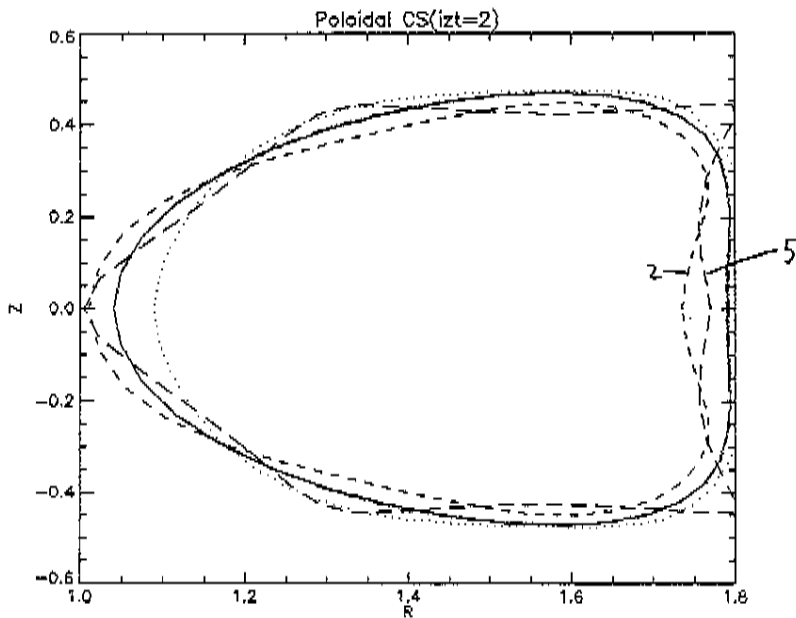
$N_{fp} \beta = 0 :$



$N_{fp} \beta = \pi/2 :$



$N_{fp} \beta = \pi :$

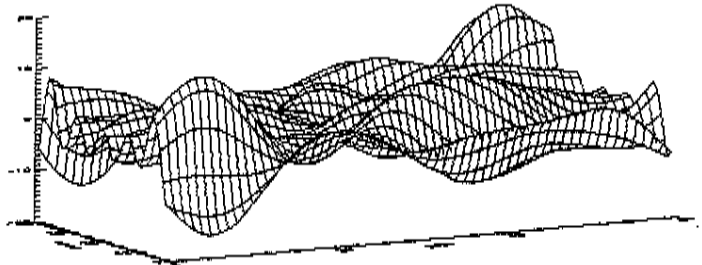
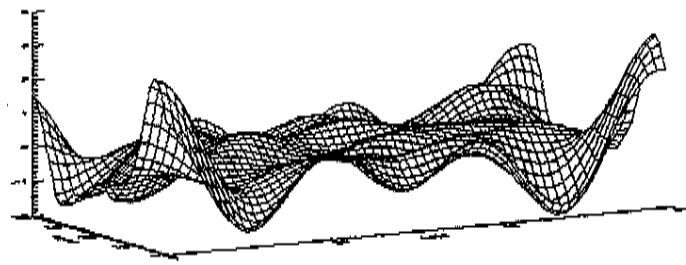
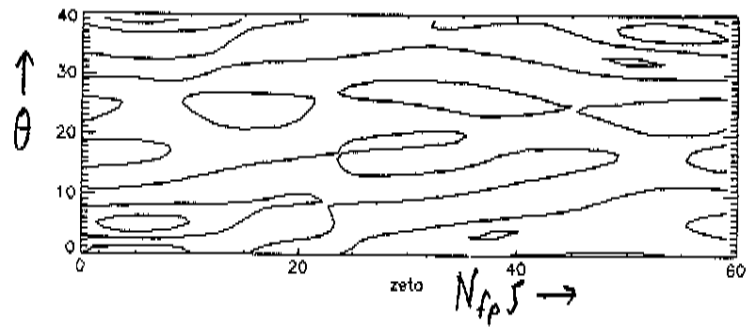
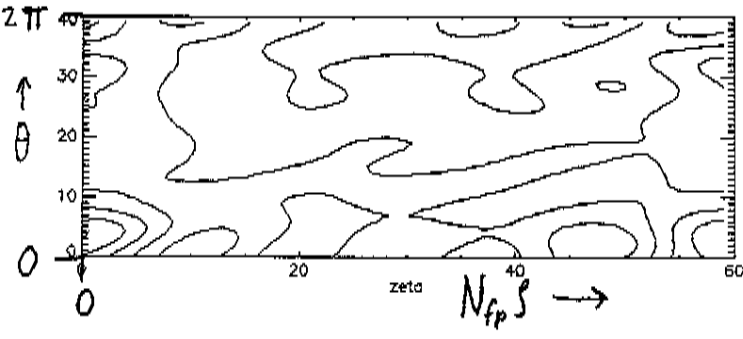


	i	
unpert = 0		— (c10)
$\delta \chi_1^2$	1
$\delta \chi_2^2$	2	-----
δW_1	3	-.-.-.-.
δW_2	4
$\delta \lambda_{\text{Kink}}$	5	-----

(B) 'Less-constrained' case ($M_p=2$):

- Plot $\xi^{(i)}(\theta, \zeta)$:
 $i=1$ (χ^2)

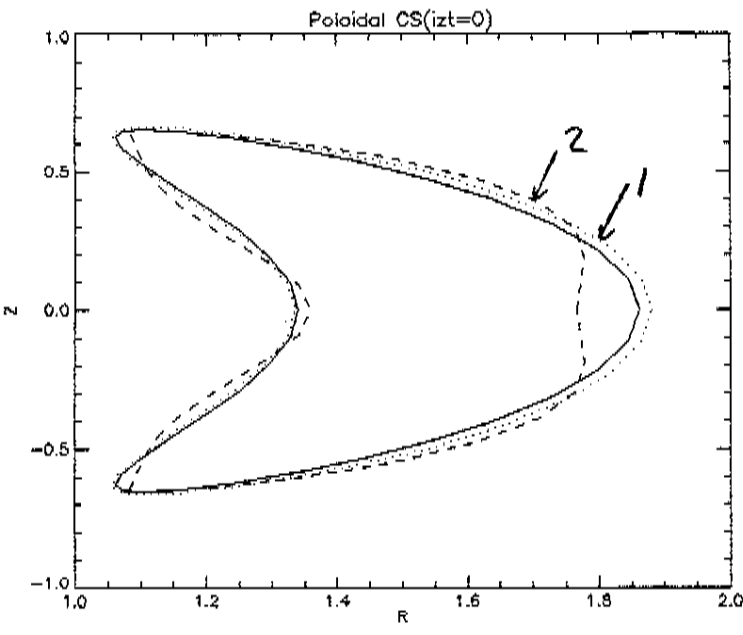
$i=2$ (λ_{-kinK})



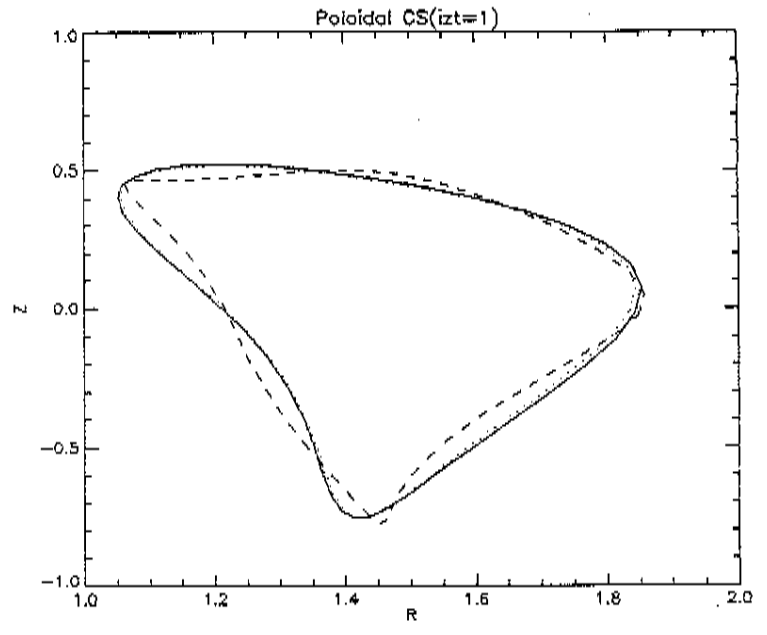
L

(B), cont:

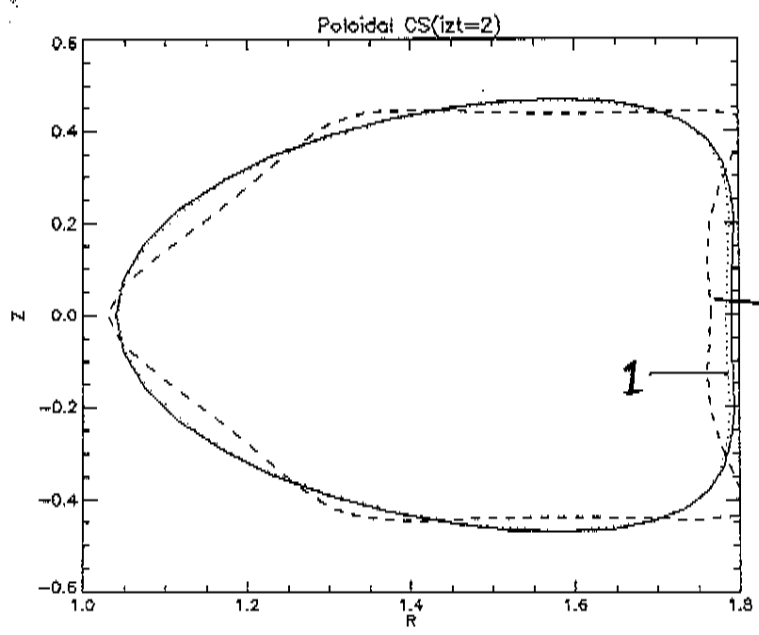
$N_{fp} \int = 0 :$



$N_{fp} \int = \pi/2 :$



$N_{fp} \int = \pi :$

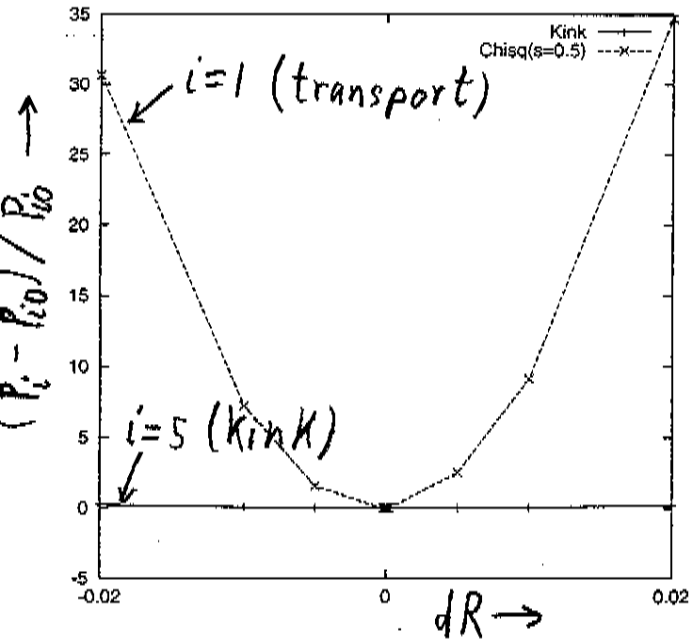


\underline{L}
 unpert = 0 ——— (c10)
 1
 2 - - - -

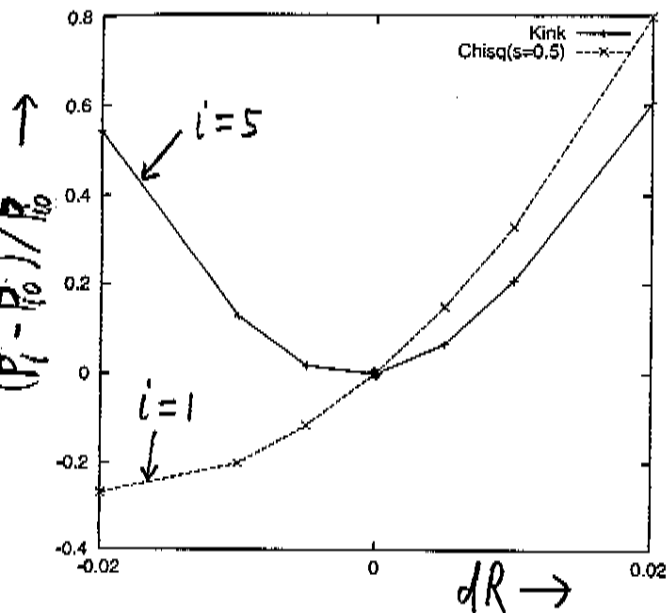
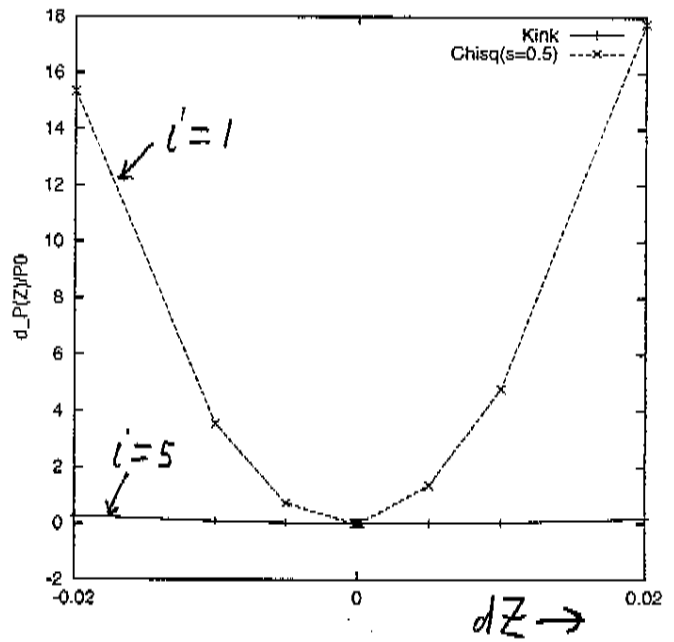
(note indentedness)

• Topography of Z-space:

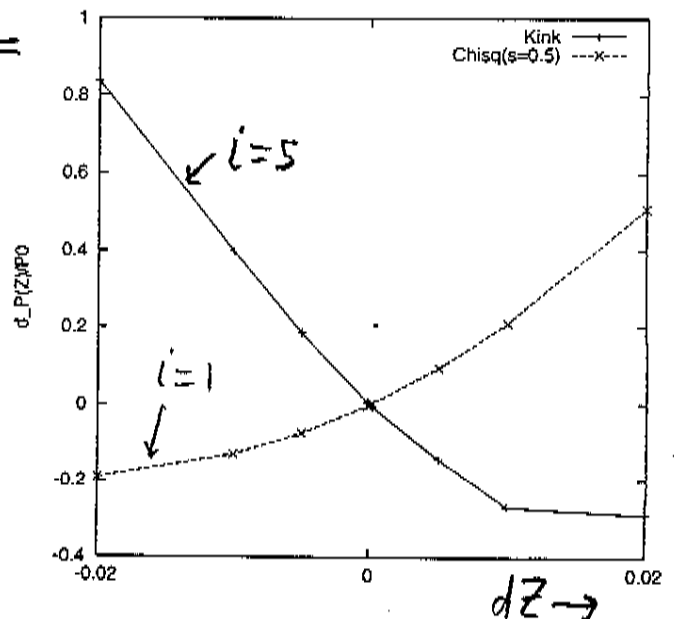
The validity of Eqs. (1) or (2) depends on the typical scales of variation in X- or Z-space of the P_i . We have assessed this variation for all 78 X_j for the P_i presently being used, in the vicinity of the $X_0 = c10-c82$ family of configurations. Some typical results:



$(\tilde{n}, m) = (-3, 1)$

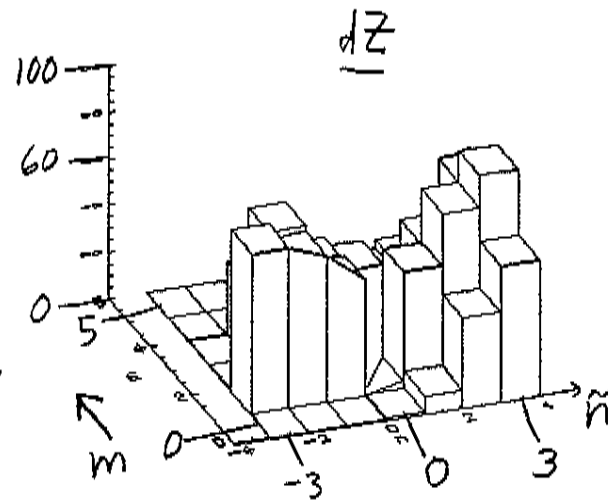
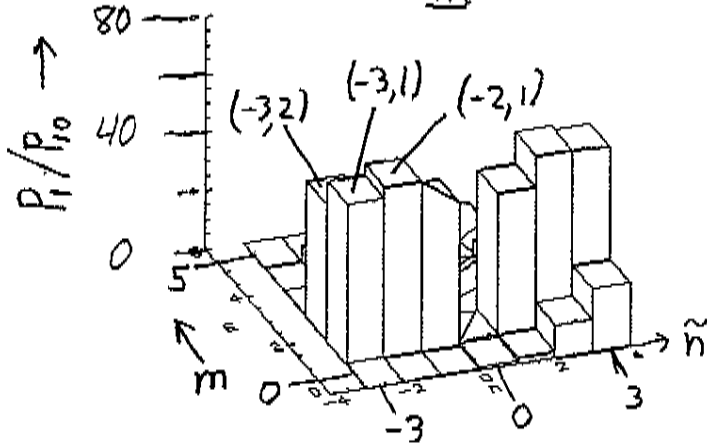


$(\tilde{n}, m) = (1, 5)$

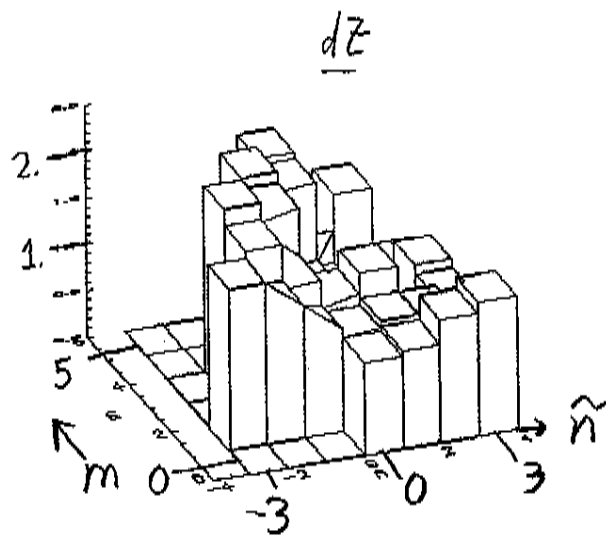
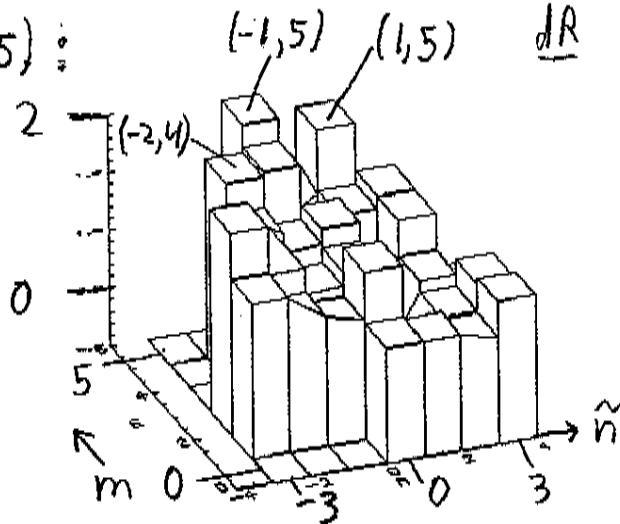


● Histograms of sensitivity over (\tilde{n}, m) -plane:

$(i=1):$ dR



$(i=5):$ dR



•Trends:

•As for the ξ^i , the dominant \mathbf{m} are similar for $i = 1 - 4$, and different from those for $i = 5$. Because of the symmetrizing action of the optimizer in creating c10, for almost all \mathbf{m} , the fractional changes p_i/p_{0i} for transport ($i = 1, 4$) are much larger than that ($i = 5$) for kink stability.

•The linear approximation Eq.(2) is valid only for fairly small displacements \mathbf{z} (~ 1 millimeter) for some Z_j . However, the quadratic form (1) appears a good approximation for perturbations \mathbf{z} on the order of a few centimeters. The simple \mathbf{Z} -space topography in the vicinity of c10 suggests that we can obtain a highly tractable model for study in this region. *E.g.*, from Eq.(1) one can compute the control matrix for *any* \mathbf{Z} in this region:

$$G_{ij}(\mathbf{Z}) \equiv \partial p_i(\mathbf{Z})/\partial z_j = G_{ij}(\mathbf{Z}_0) + H_{ijk}z_k, \quad (3)$$

and from this, find the correct ξ^i at any \mathbf{Z} , along with the extrema of the P_i , *etc.*

⇒ Here, we will present a 1st calculation of both G_{ij} and H_{ijk} around the c10 design point, within a 'reduced model' having $N_z \ll N_x$, and demonstrate numerically the 'proof of principle' of the CM method for this model.

● Reducing the dimensionality of Z:

● The dimensionality $N_x = N_z$ of the search space used up to now and $N_x - M_p$ of its null subspace are large (78 and 73, resp.). The smaller we can make these, the better. Here, we shall reduce N_z by 2 general methods:

(a) Removing the redundancy in the X-specification. This reduces N_z from $N_x = 78$ to $N_x/2 = 39$.

(b) Taking only the perturbations most effective in varying some P_i . Here, we choose the 4 most effective for P_1 , and for P_5 , thus further reducing N_z from 39 to 8.

● On method (a): For the calculations presented so far, each R_m and Z_m harmonic is independently varied. However, these variations are not, in fact, independent since the poloidal angle variable is not uniquely defined. Such redundancy in the representation contributes extra nonphysical dimensions to the null space. In calculating the Control and Hessian matrices [Eq.(1)] we should use the $N_z \sim N_x/2$ linear combinations of the R_m, Z_m that define normal displacements to the plasma boundary.

● Defining normal displacements to the plasma boundary:

For a plasma boundary defined by

$$\vec{X}(\theta, \phi) = R(\theta, \phi)\hat{R}(\phi) + Z(\theta, \phi)\hat{Z}, \quad (4)$$

a general displacement is $\vec{\xi} = \delta\vec{X} = \delta R\hat{R} + \delta Z\hat{Z}$, and a normal displacement is

$$\vec{\xi} \cdot \frac{\partial \vec{X}}{\partial \theta} \times \frac{\partial \vec{X}}{\partial \phi} = R \left(\frac{\partial R}{\partial \theta} \delta Z - \frac{\partial Z}{\partial \theta} \delta R \right). \quad (5)$$

Multiplying by $\cos(m\theta + n\phi)$ and integrating over θ and ϕ yields a matrix equation in the form

$$\xi_i = \sum_j B_{ij} \delta_j. \quad (6)$$

Here $\delta_j (j = 1, \dots, N)$ is the set of Fourier expansion coefficients of both δR and δZ , $\xi_i (i = 1, \dots, M)$ is the set of Fourier coefficients of the normal displacement to the plasma boundary, and B_{ij} is the $M \times N$ rectangular influence matrix that relates the two. Our goal is to calculate the δ_j since these are required by VMEC.

An SVD decomposition of the matrix B is

$$B_{M \times N} = U_{M \times N} \Sigma_{N \times N} V_{N \times N}^T \quad (7)$$

where U and V are orthogonal matrices and Σ is a diagonal matrix of singular values σ_k . In terms of the decomposition a solution to Eq. 6 is conveniently written as

$$\delta_i = \sum_{k=1}^N V_{ik} t_k \quad (8)$$

where

$$\begin{aligned} t_k &= \sigma_k^{-1} \sum_{j=1}^M U_{jk} \xi_j & \text{if } \sigma_k > 0, \\ &= 0 & \sigma_k < \sigma_{cutoff} \approx 0 \end{aligned} \quad (9)$$

It is convenient to rewrite Eq. 8 in the equivalent vector form

$$\vec{\delta} = \sum_{k=1}^N t_k \vec{v}_k \quad (10)$$

where \vec{v}_k is the k 'th column (vector) of matrix V . Suppose we order the singular values in descending order such that

$$\begin{aligned} \sigma_k &> 0 & \text{for } k = 1, 2, \dots, N_s \\ \sigma_k &= 0 & \text{for } k = N_s + 1, \dots, N \end{aligned} \quad (11)$$

Then

$$\vec{\delta} = \sum_{k=1}^{N_s} t_k \vec{v}_k \quad (12)$$

provides a complete description of an arbitrary normal perturbation of the plasma boundary. The t_k are given by Eq. 9.

Now consider a specific normal displacement $\vec{\xi} \equiv \vec{\xi}^{(\ell)} = \vec{e}_\ell$, where

$$\vec{e}_\ell = [0, 0, \dots, 1, 0, \dots, 0]^T \quad (13)$$

with the “1” in the ℓ 'th entry. Thus $\vec{\xi}^{(\ell)}$ corresponds to a pure harmonic of the normal displacement with modenumbers $m(\ell), n(\ell)$. From Eq. 12 this $\vec{\xi}^{(\ell)}$ corresponds to a vector of $\delta R_{m,n}, \delta Z_{m,n}$ displacements which we can write as

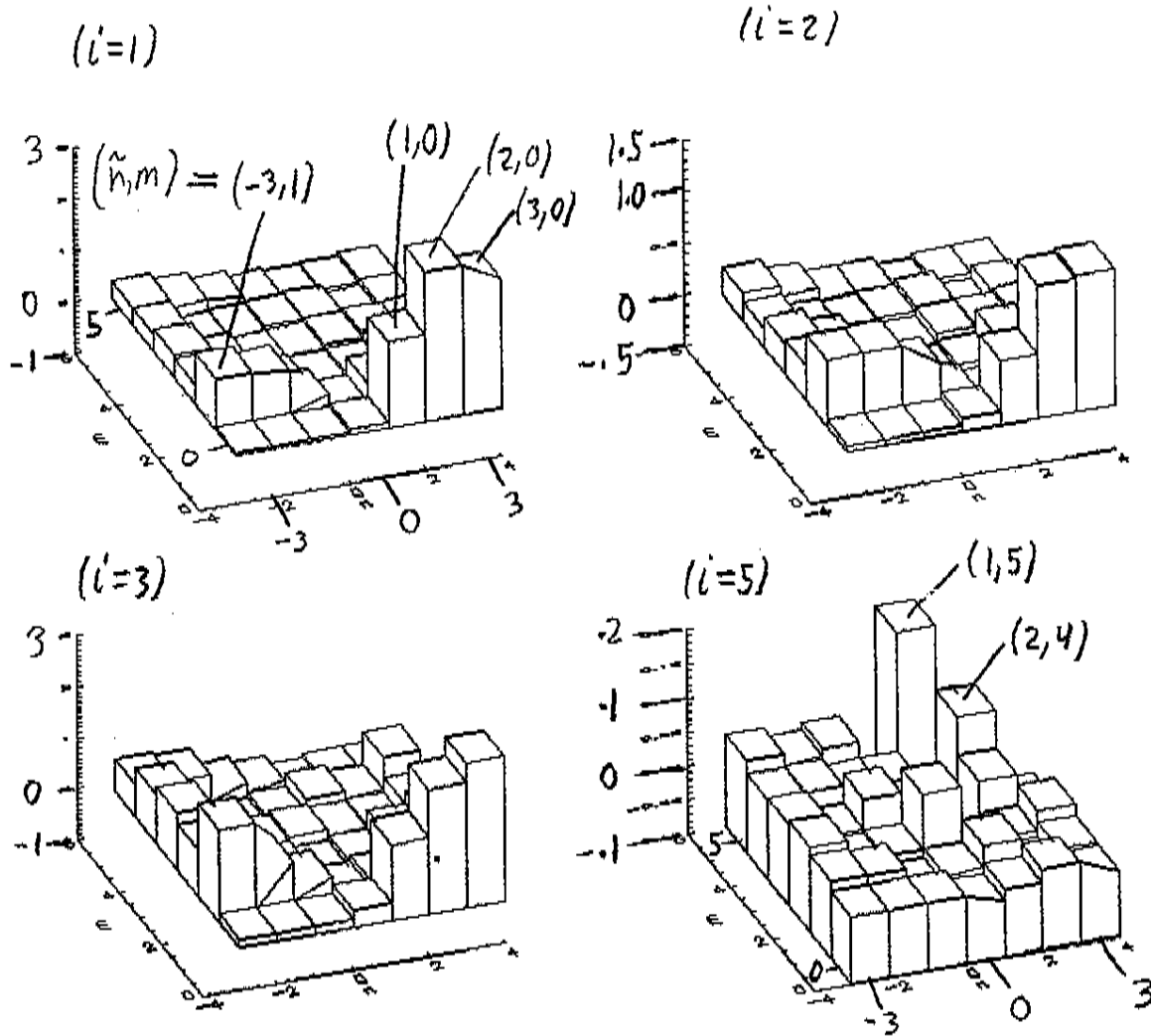
$$\vec{\delta}^{(\ell)} = \sum_{k=1}^{N_s} t_k^{(\ell)} \vec{v}_k$$

with

$$t_k^{(\ell)} = \frac{1}{\sigma_k} U_{\ell k}. \quad (14)$$

The vectors $\vec{\delta}^{(\ell)}$ are the displacement vectors used to form the control and quality matrices.

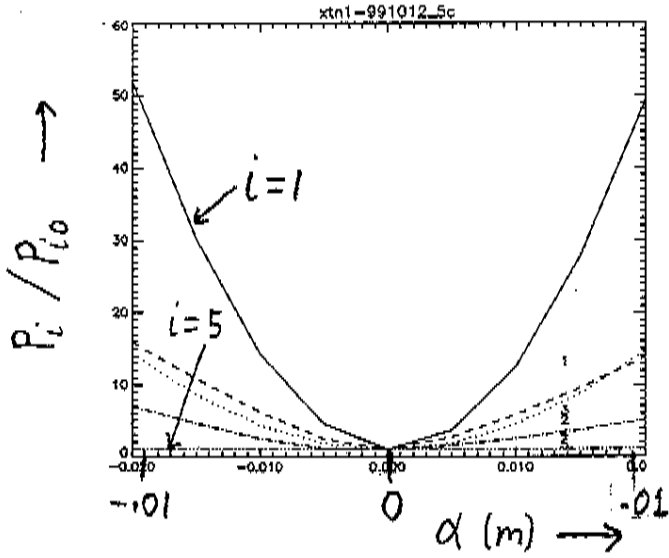
- Reduced Model & 1st Calculation of G_{ij} , H_{ijk} :
- Sensitivity histograms in the $N_z = 39$ Z-space:



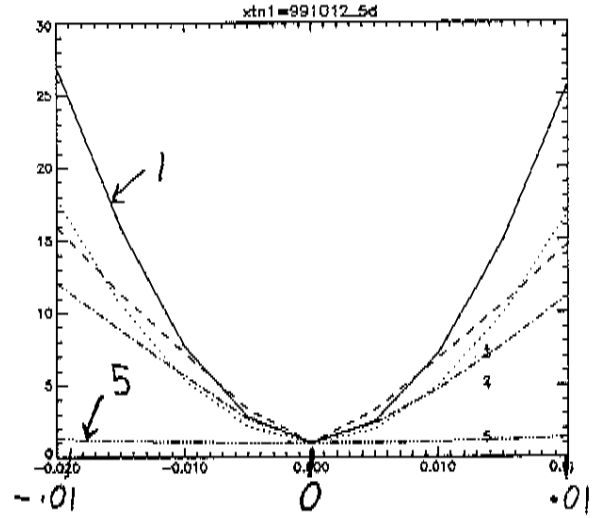
- Ranking $|P_i/P_{i0} - 1|$, select 4 most effective harmonics m for each of $i = 1, 5$:
- For P_1 : $(\tilde{n}, m) = \{(1, 0), (2, 0), (3, 0), (-3, 1)\}$
- For P_5 : $(\tilde{n}, m) = \{(1, 3), (1, 4), (2, 4), (1, 5)\}$.

• Topography of reduced space •

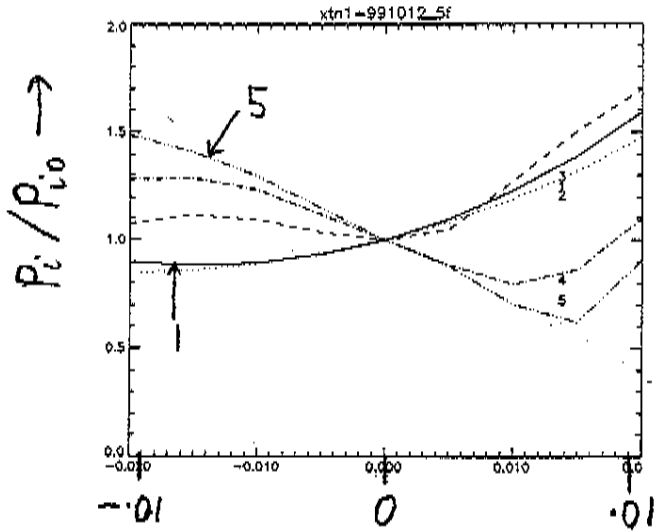
$j = 1, m_j = (1, 0)$



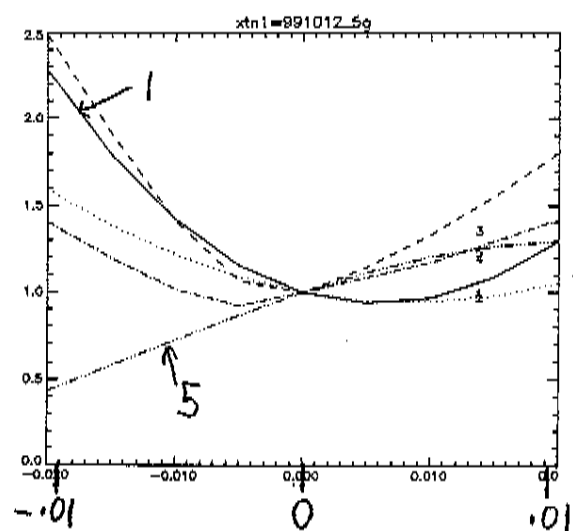
$j = 4, m_j = (-3, 1)$



$j = 5, m_j = (1, 3)$



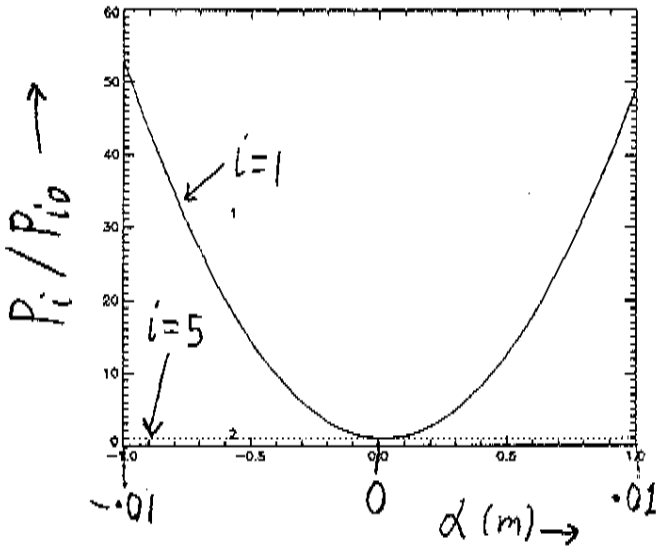
$j = 7, m_j = (2, 4)$



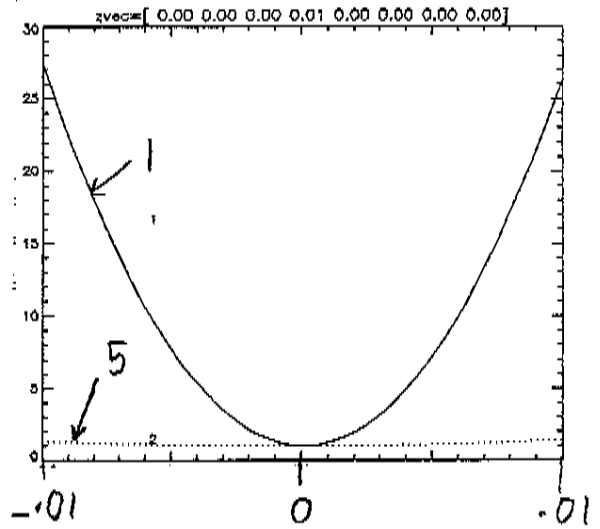
● Distill $G_{ij}, H_{ijk} \Rightarrow$ 'Quadratic Model'
for $N_z = 8$: (Requires $2N_z^2 = 128$ perturbed equilibria about Z_0 .)

● Compare this semi-analytic model with numerical results just shown:

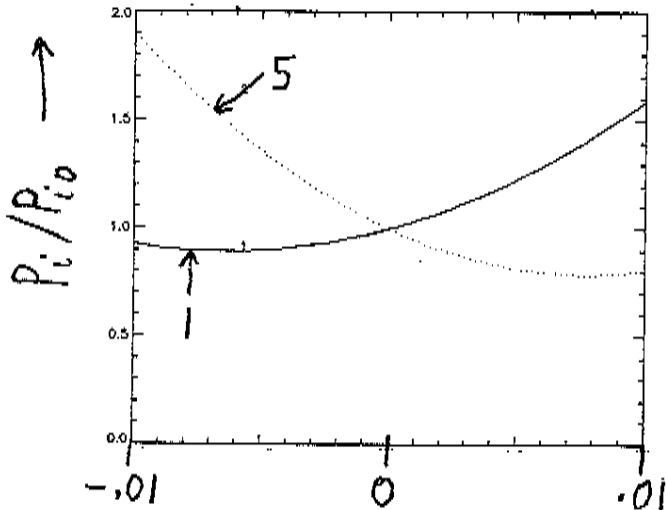
$j=1, m_j = (1,0)$



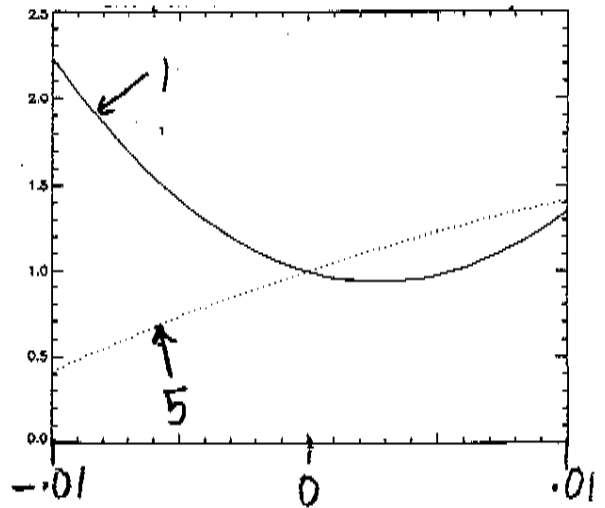
$j=4, m_j = (-3,1)$



$j=5, m_j = (1,3)$

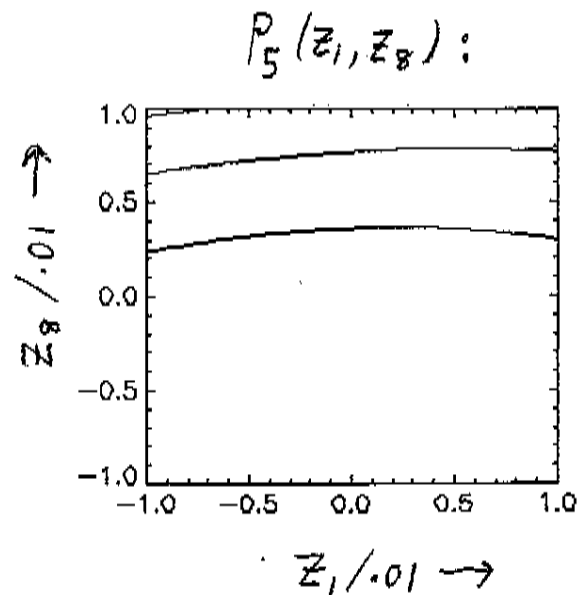
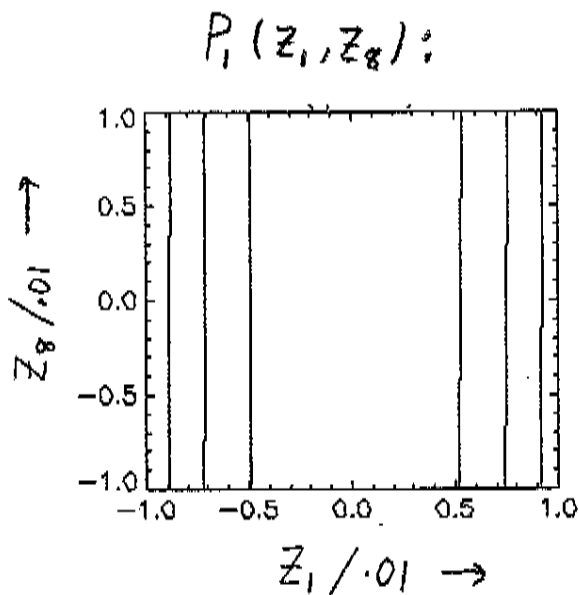
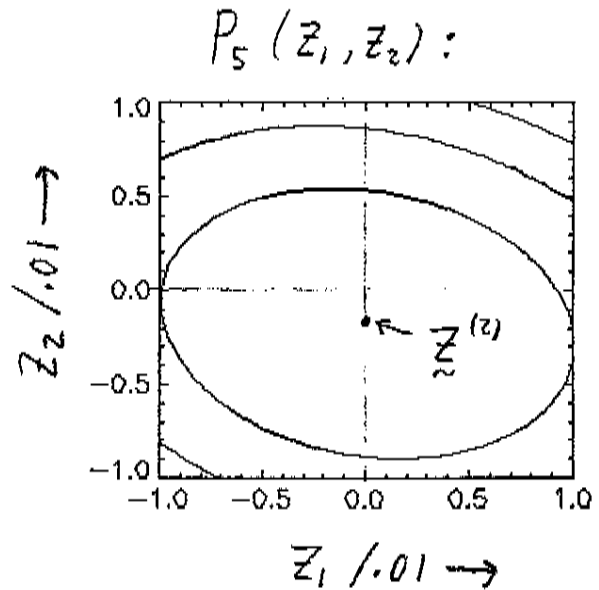
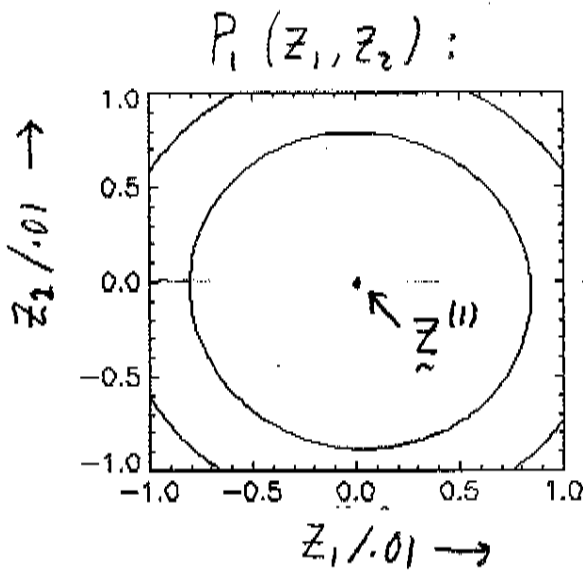


$j=7, m_j = (2,4)$



• Use Quadratic Model to analyse **Z**-space structure, compute ξ^i 's, etc.:

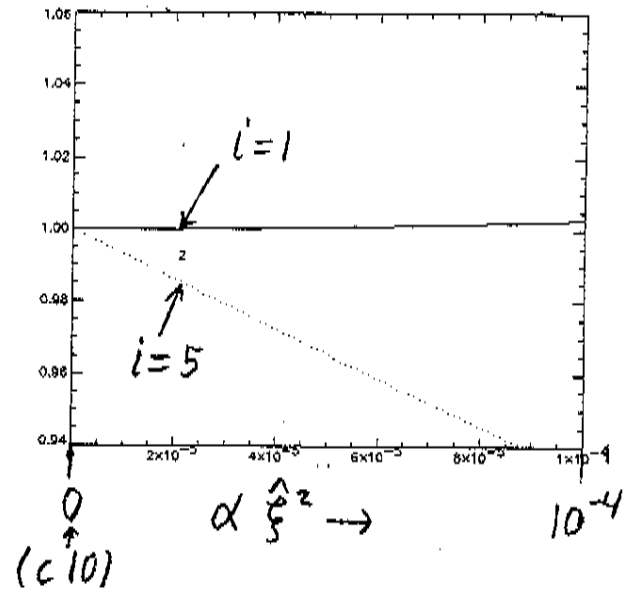
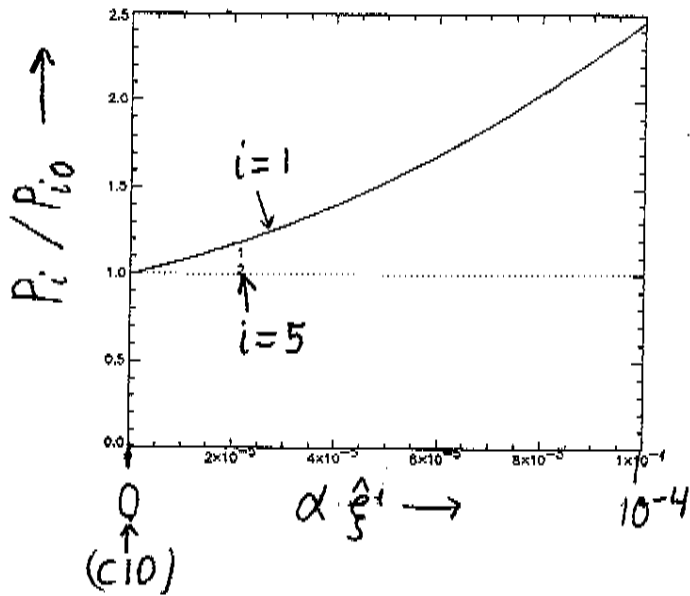
• Plot $P_{1,5}$ versus pairs (z_{j1}, z_{j2}) :



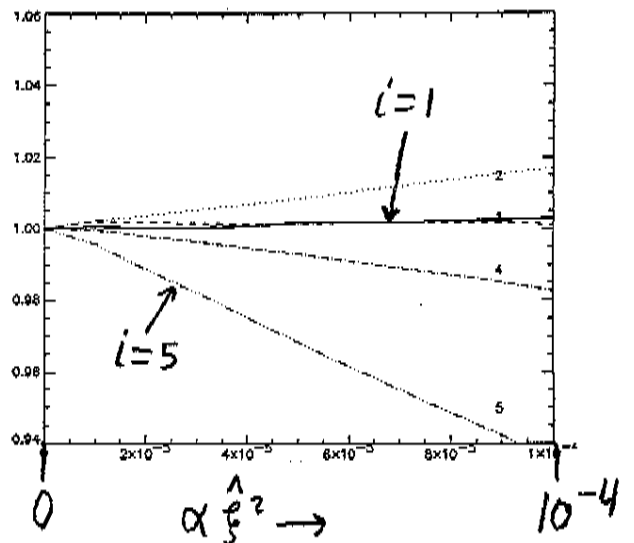
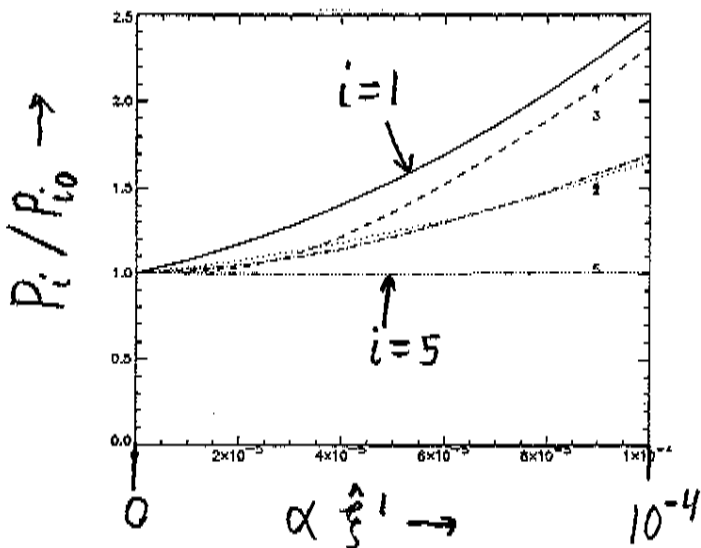
• (Note : z_1, z_8 almost perform job of ξ^1, ξ^5 , viz, varying P_1, P_5 independently.)

• ‘Proof of Principle’ of CM method:

• Plot P_i versus $\alpha \xi^{j=1,5}$, verifying their independent control of $P_{1,5}$:



• Compare with numerical results from perturbed equilibria:



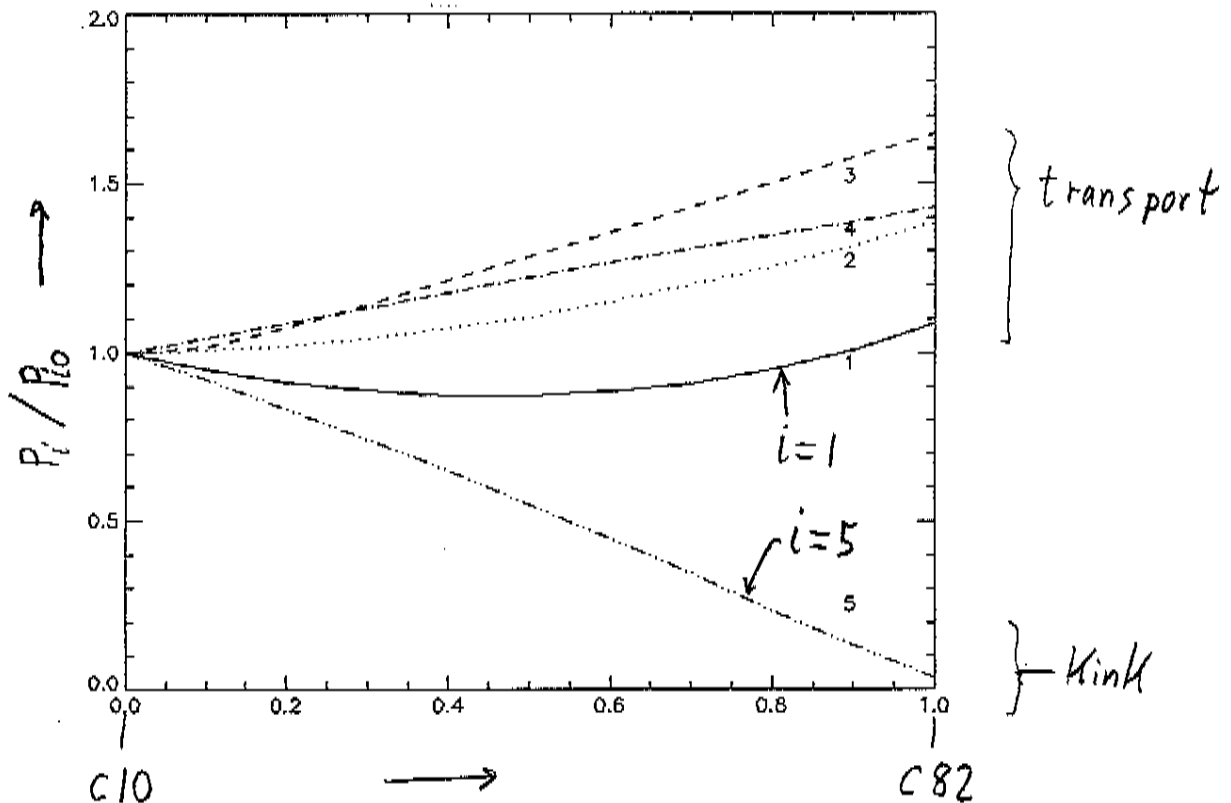
● Other QAS Design Points:

● c10 was arrived at along an involved path of human interaction with the optimizer, and it is unclear that other regions of **Z**-space, which would have been reached from different starting points, might not yield superior configurations. Thus, we are starting to study other proposed QAS configurations^{2,3} with the same methods, and to consider the variation of the P_i as one moves from one such point Z_0 to another.

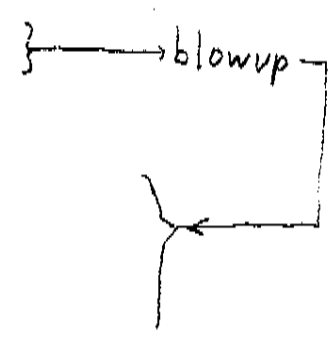
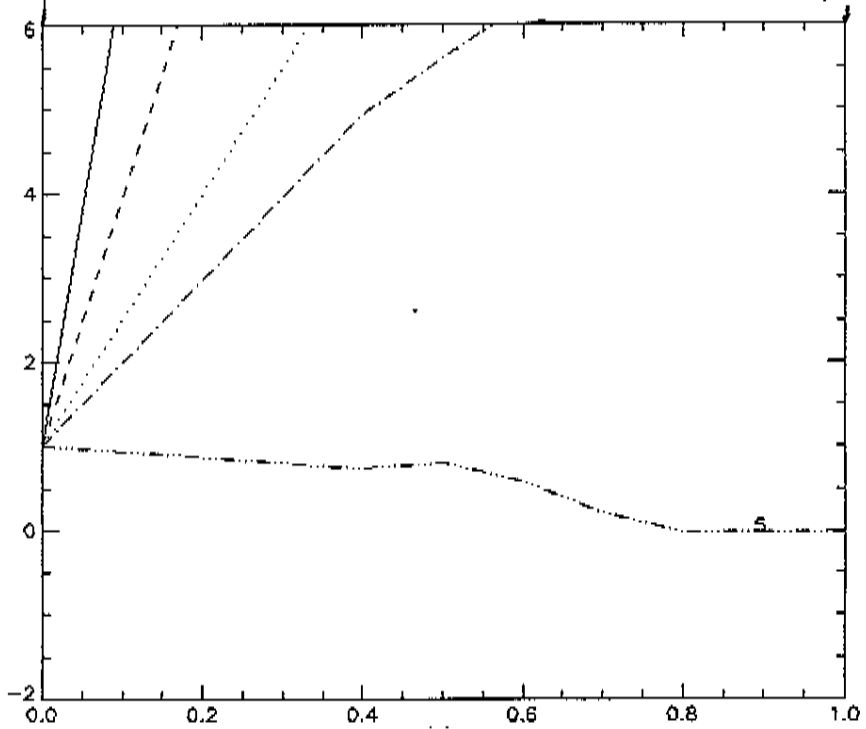
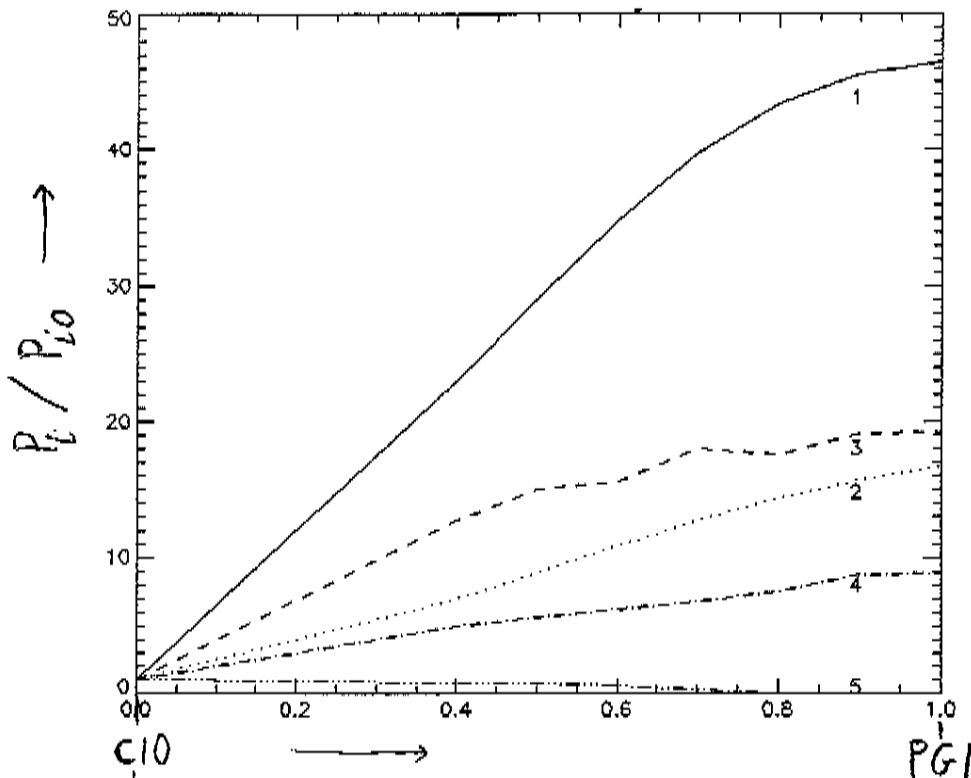
● Warmup (**Z**'s nearby): The path c10 → c82:

● c82 was obtained from c10 in an effort to stabilize the kink. The level of QA-ness was slightly degraded in compensation. This borne out by the P_i 's along a straight-line path in **Z**-space:

$$|\sum_{i=1}^5 P_{i,c82} - \sum_{i=1}^5 P_{i,c10}| \approx .041 m$$



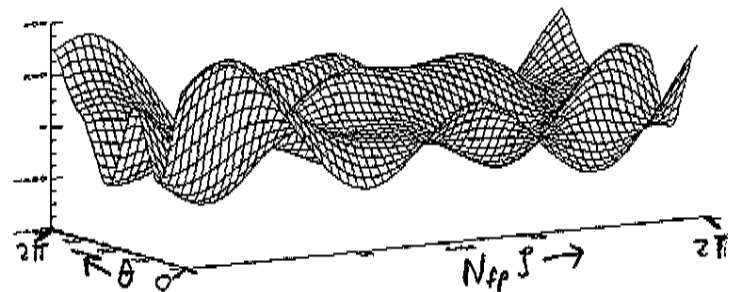
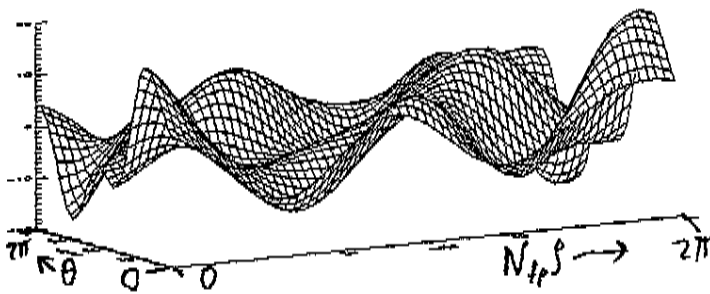
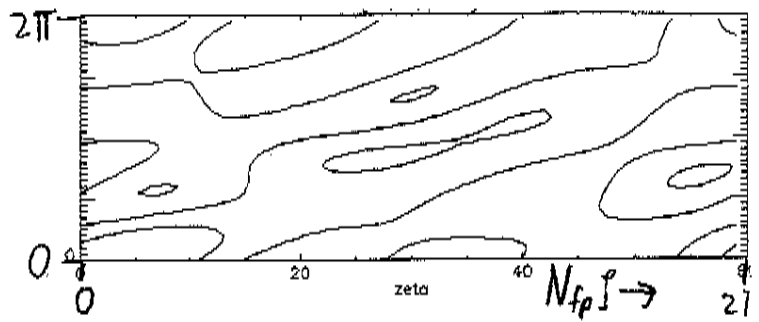
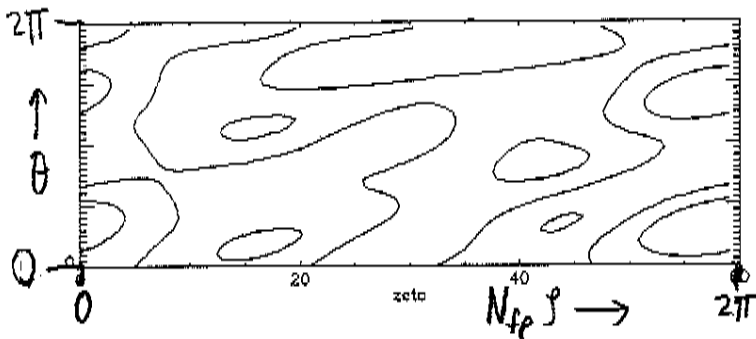
- The path c10 \rightarrow PG1 (preliminary):
- Define norm $|\underline{X}| \equiv [\sum_j X_j^2]^{1/2}$, $|\underline{X}_{PG1} - \underline{X}_{c10}| \approx .228$ m
- PG1 characterized by much better kink stability, substantially worse QA-ness (mainly due to large mirror field $B_{m=0, \tilde{n}=1}$ present to enhance stability).



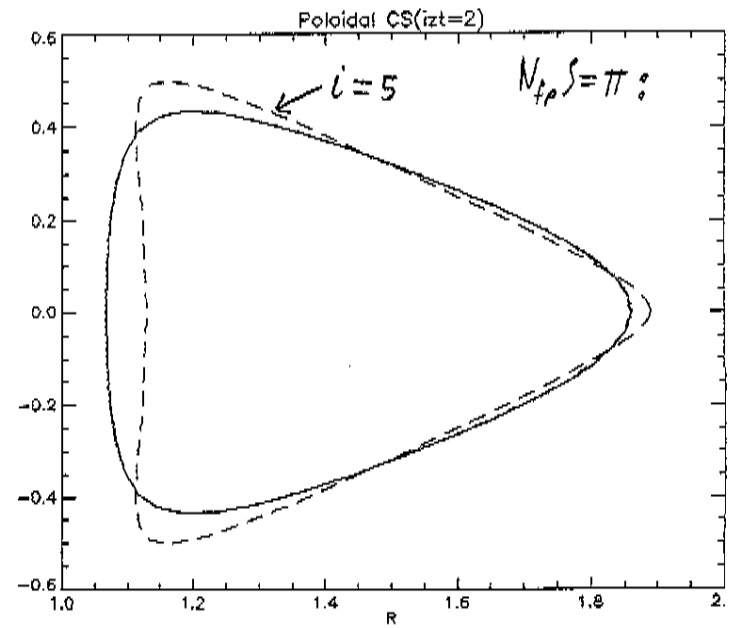
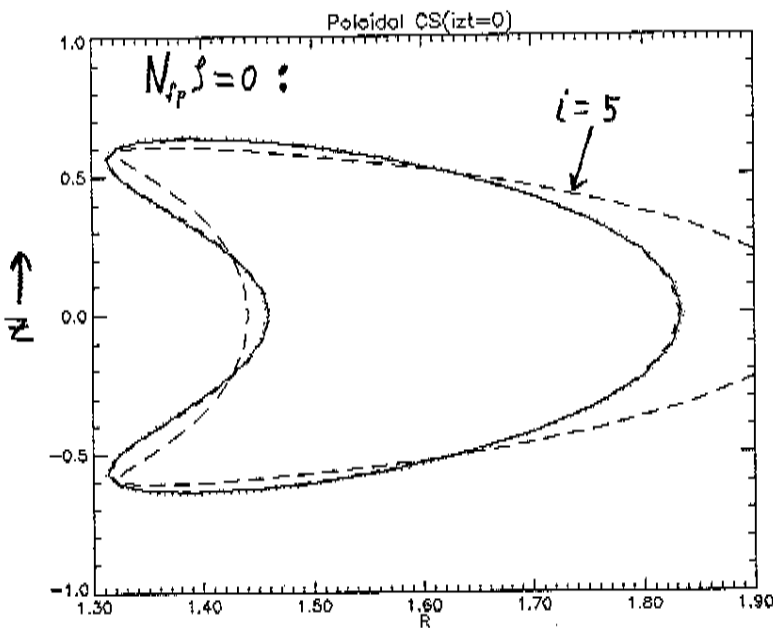
● PG1: preliminary results:

● For $M_p = 5$:

● Not as much difference discernable between the transport and kink $\xi^i(\theta, \zeta)$:



● Kink perturbation again enhances the triangularity at $N_{fp}\zeta = \pi$, which is positive for PG1, consistent with tokamak-based intuition:



● Summary:

- We have set up the machinery needed to do the indicated CM analysis of NCSX, and have provided a 1st demonstration of the basic principle of the CM method, showing for c10 that the SVD-obtained perturbations ξ^i can in fact be used to vary the P_i independently.
- For the 1st time, we have provided a picture of the topography of the configuration space \mathbf{X} or \mathbf{Z} in which our searches for good stellarators are occurring. In an appreciable neighborhood of c10, the P_i may be modeled by a quadratic function of $\mathbf{z} = \mathbf{Z} - \mathbf{Z}_0$, and vary with little structure even over a scale comparable to the distance from c10 to PG1. We have constructed this quadratic representation about c10 for a reduced set ($N_z = 8$) of perpendicular displacements of the c10 boundary, computing both the CM G_{ij} and Hessian H_{ijk} for this set.
- The 4 different transport figures of merit produce boundary displacements $\xi^i(\theta, \zeta)$ similar in appearance. However, the G-matrix eigenvalues w_i show these are linearly independent, NOT nearly collinear.
- The $\xi^{i=5}$ for kink stability differs in appearance

from those for transport. For c10, ξ^5 provides the outboard indentation previously seen to stabilize the kink, enhancing c10's negative triangularity at $N_{fp}\zeta = \pi$, while for PG1, ξ^5 enhances its *positive* triangularity, consistent with tokamak intuition on kink stabilization.

- We have reduced the dimensionality N_z of the search space from $N_x = 78$ to $N_z = 8$ of the reduced model by 2 means:
 - (a) Removing the redundancy in the **X**-specification.
 - (b) Taking the perturbations most effective in varying P_i 's of interest.

We intend to refine method (b), with the goal of expressing the physics characteristics of these stellarators in terms of a relatively modest set of parameters, which should aid in both our understanding, and in focussing the optimizer.

- The same approach will be used to study how a given set of coils (with perturbations $\delta\mathbf{I}$) could produce a range of physics behavior π for experimental flexibility:

$$\mathbf{G} \cdot \boldsymbol{\xi} = \pi \text{ (as above),}$$

$$\mathbf{C} \cdot \delta\mathbf{I} = \boldsymbol{\xi} \text{ (from free-boundary runs),}$$

$$\Rightarrow \mathbf{G}_2 \cdot \delta\mathbf{I} = \pi, \text{ with } \mathbf{G}_2 \equiv \mathbf{G} \cdot \mathbf{C}.$$

References

- ¹A. Reiman, G. Fu, S. Hirshman, D. Monticello, H. Mynick, *et al.*, European Physical Society Meeting on Controlled Fusion and Plasma Physics Research, Maastricht, the Netherlands, June 14-18, 1999, (European Physical Society, Petit-Lancy, 1999).
- ²M.Yu. Isaev, M.I. Mikhailov, D.A. Monticello, H.E. Mynick, A.A. Subbotin, L.P. Ku, A.H. Reiman, *Phys. Plasmas* **6** 3174 (1999).
- ³N. Nakajima, M. Yokoyama, M. Okamoto, J. Nührenberg, *Plasma Physics Reports* **23**, 460 (1997).
- ⁴P. Garabedian, L.P. Ku, *Phys. Plasmas* **6**, 645 (1999).